Stress-Induced Mutagenesis Breaks the Trade-Off Between Adaptability and Adaptedness

Yoav Ram and Lilach Hadany

Email: YR - yoavram@post.tau.ac.il, LH - lilach.hadany@gmail.com

Address: Dept. of Molecular Biology and Ecology of Plants, Tel Aviv University Tel-Aviv 69978, Israel. Tel. +972.3.640.6886

Running title: SIM, adaptability, and adaptedness

Keywords: adaptation, fitness, models/simulations, mutations, population genetics, trade-offs

Online elements: Supporting Text, Figure S1, Figure S2, Figure D1, Figure E1, Figure E2, Figure F, color version of figure 2, color version of figure 3, color version of figure 4, IPython notebook for figure reproduction.

Manuscript type: article

Abstract

Because mutations are mostly deleterious, mutation rates should be reduced by natural selection. However, mutations also provide the raw material for adaptation. Therefore, evolutionary theory suggests that the mutation rate must balance between *adaptability* – the ability to adapt – and *adaptedness* – the ability to remain adapted. We model an asexual population crossing a fitness valley and analyze the adaptation rate with and without stress-induced mutagenesis – the increase of mutation rates in response to stress or maladaptation. We show that stress-induced mutagenesis breaks the evolutionary trade-off between *adaptability* and *adaptedness*, increasing one without reducing the other. Our theoretical results support the hypothesis that stress-induced mutagenesis promotes adaptation and provide quantitative predictions of the adaptation rate with different mutational strategies.

1. Introduction

There is experimental, clinical and theoretical evidence that high mutation rates increase the rate of adaptation and that during adaptive evolution, constitutive mutators - alleles that constitutively increase the mutation rate - can rise in frequency because of the beneficial mutations they generate (reviewed in Sniegowski et al. 2000; de Visser 2002; Denamur and Matic 2006). However, during evolution in a stable environment, constitutive mutators become associated with poor genetic backgrounds due to increased accumulation of deleterious mutations; this was evidenced both in the lab (Funchain et al. 2000) and in the clinic (Montanari et al. 2007). Classical models suggest the "reduction principle", which states that natural selection reduces the mutation rate in a stable environment (Kimura 1967; Liberman and Feldman 1986). But many adaptations require new beneficial mutations, especially in asexual populations. This tension between the effects of beneficial and deleterious mutations leads to "the rise and fall of the mutator allele" (Giraud et al. 2001b), where mutator alleles increase in frequency in a maladapted population, only to be eliminated by natural selection when the population is well-adapted. This dynamic was studied using experimental evolution (Sniegowski et al. 1997; Wielgoss et al. 2012), mathematical analysis, and simulations (Taddei et al. 1997; Kessler and Levine 1998; Tenaillon et al. 1999).

Thus, the mutation rate must balance between two evolutionary traits, as Leigh (1970) suggested: *adaptability* – the capacity to adapt to new environmental conditions – and *adaptedness* – the capacity to remain adapted to existing conditions.

Stress-induced mutagenesis (SIM) - the increase of mutation rates in stressed or maladapted individuals - has been demonstrated in several species, including both prokaryotes and eukaryotes (Galhardo et al. 2007). SIM has been observed in lab strains (Foster 2007; Rosenberg et al. 2012) and natural populations of *Escherichia coli* (Bjedov et al. 2003; but also see Katz and Hershberg 2013), and in other species of bacteria such as Pseudomonads (Kivisaar 2010), *Helicobacter pylori* (Kang et al. 2006), *Vibrio cholera* (Baharoglu and Mazel 2011) and *Streptococcus pneumonia* (Henderson-Begg et al. 2006). SIM has also been observed in yeast (Heidenreich 2007; Rodriguez et al. 2012), algae (Goho and Bell 2000), nematodes (Matsuba et al. 2012), flies (Sharp and Agrawal 2012), and human cancer cells (Bristow and Hill 2008). Several stress responses regulate the mutation rate in bacteria by shifting replication to error-prone DNA polymerases (Ponder et al. 2005) and by inhibiting the mismatch repair system (Debora et al. 2010). These stress responses include the SOS DNA-damage response, the RpoS-controlled general or starvation stress response, and the RpoE membrane protein stress response (Al Mamun et al. 2012).

It is still not clear how SIM affects evolution and adaptation. Some authors have proposed that SIM has a significant impact on *adaptability* or *evolvability* (Tenaillon et al. 2004; Cirz and Romesberg 2007; Rosenberg et al. 2012), but there is no theoretical treatment of this impact. On the other hand, the effect of SIM on *adaptedness* was studied with deterministic (Agrawal 2002) and stochastic (Shaw and Baer 2011) models. These works showed that without beneficial mutations SIM doesn't affect the mean fitness of asexual populations in stable environments, in contrast with constitutive mutagenesis, which decreases the population mean fitness. More

recently, we have shown that with rare beneficial mutations, if maladapted individuals increase their mutation rate then the population mean fitness of asexual populations increases (Ram and Hadany 2012).

Here, we analyze population genetics models of adaptive evolution to explore the rate of adaptation on a rugged fitness landscape, in which adaptations require two separately deleterious mutations (Wright 1931; Wright 1988). We develop analytic approximations and stochastic simulations and compare normal, constitutive, and stress-induced mutagenesis. We show that stress-induced mutagenesis can break the trade-off between *adaptability* and *adaptedness* by increasing the adaptation rate without decreasing the population mean fitness.

2. Model

We model a population of N haploid asexual individuals with a large number of loci in full linkage. The model includes the effects of mutation, selection, and genetic drift. Individuals are characterized by their genotype in two specific bi-allelic loci – *ab*, *Ab*, *aB*, and *AB* – and by the number of deleterious mutations they carry in the rest of the non-specific loci. For example, *aB*/*3* is the *aB* genotype with additional three deleterious mutations in non-specific loci.

We focus on adaptation to a new environment. The fitness of the wildtype *ab*/*0* is 1, the fitness of the single mutants *Ab*/0 and *aB*/0 is 1-s, and the double mutant *AB*/*0* has the highest fitness 1+sH, where s is the selection coefficient and H is the relative advantage of the double mutant. This is the simplest case of a "rugged fitness

96 landscape": the single mutants *Ab* and *aB* are fitness "valleys" between the local and
97 global fitness "peaks" *ab*/0 and *AB*/*0* (Figure 1).

98

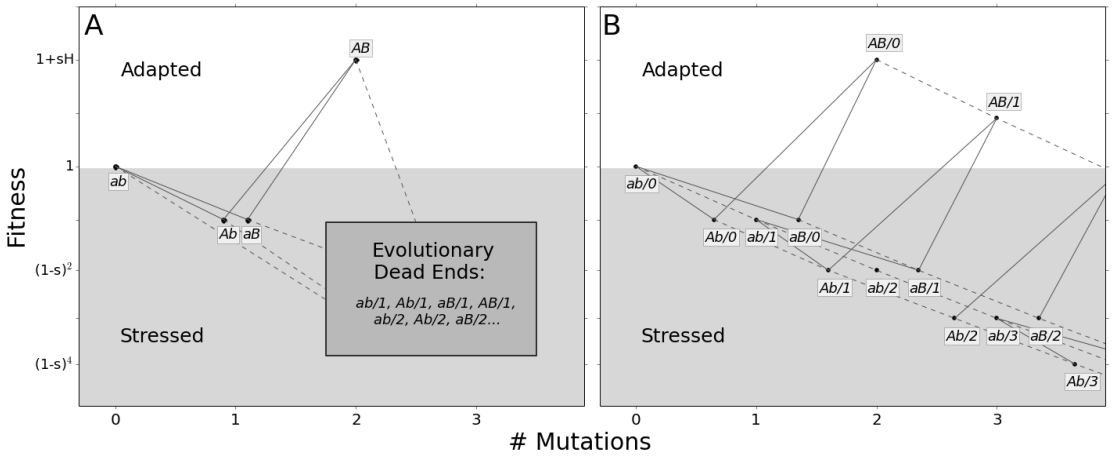

99

100 **Figure 1 – Adaptation on a rugged fitness landscape.** The figure shows the fitness of the
101 possible genotypes: *ab*, or *Ab*, *aB*, and *AB*. Panel B also includes the number of deleterious
102 alleles across the genome following the forward-slash ('/'). The y-axis represents fitness: the
103 wildtype *ab*/*0* has fitness 1; the fittest genotype *AB*/0 has fitness 1+*sH*; deleterious alleles,
104 either at the *A*/*a* and *B*/*b* loci, or at the non-specific loci, reduce fitness by 1-*s*. The x-axis
105 represents the number of accumulated mutations. Solid lines represent mutations at the *a*/*A*
106 and *b*/*B* loci, occurring with probability μ. Dashed lines represent deleterious mutations in the
107 rest of the genome, occurring with rate *U*. Mutagenesis is induced in stressed genotypes with
108 fitness <1 (gray background). Fit genotypes, with fitness ≥1, do not hypermutate (white
109 background). **(A)** In the analytic model genotypes with deleterious alleles in non-specific loci
110 are considered "Evolutionary Dead Ends" and do not contribute to adaptation. **(B)** In the
111 simulations individuals can accumulate up to 25 deleterious alleles (the figure only shows
112 three). Multiple mutations can occur simultaneously but are not shown for simplicity of the
113 illustration.

Each deleterious mutation in the non-specific loci independently (multiplicatively) reduces the fitness of the individual by 1-s. Mutations occur in the specific loci with probability μ and that the number of new mutations per replication in the rest of the genome is Poisson distributed with an average U. The model neglects back-mutations and compensatory mutations.

We consider three mutational strategies: normal mutagenesis (NM), where there is no increase in the mutation rate; constitutive mutagenesis (CM), where all individuals always increase their mutation rate by τ, the mutation rate fold increase; and stress-induced mutagenesis (SIM), where only stressed or maladapted individuals increase their mutation rate by τ. Individuals are considered stressed if their fitness is below a specific threshold, so stress can be caused by a deleterious mutation (either in the specific *A*/*a* and *B*/*b* loci or in non-specific loci). The main analysis assumes that the effect of SIM on the mutation rate of an individual with fitness ω is

$$U(\omega) = \begin{cases} \tau U, & \omega < 1 \\ U, & \omega \geq 1 \end{cases}. \quad (1)$$

This equation models a scenario in which an environmental change – *i.e.*, appearance of a new ecological niche or a new carbon source – provides an opportunity for adaptation without affecting the fitness of the wildtype (*ab*/*0*). We also study a different scenario in which the environmental change reduces the absolute fitness of the wildtype so that it is also stressed – see section 3.5.

We are interested in calculating the adaptation rate of a population homogenous for each of the above mutational strategies (NM, CM, or SIM). The adaptation process is

separated into two distinct stages. In the first stage, a double mutant AB appears in the population, usually in a single copy. In the second stage, the double mutant either goes to extinction or avoids extinction, increases in frequency, and goes to fixation.

We analyzed this model with two methods. The first is analytic (Figure 1A), in which we assume that: (i) genotypes with deleterious backgrounds (deleterious alleles in the non-specific loci) do not contribute to the adaptation process; and (ii) the number of deleterious alleles per individual before the appearance of a double mutant is at a mutation-selection balance (MSB) and is Poisson distributed with mean U/s (Haigh 1978). The former assumption requires that mutation is weaker than selection ($U \ll s$); the later assumption only requires that mutation is not much stronger than selection. Specifically, the expected number of mutation-free individuals is at least one: $Ne^{-U/s} > 1 \Rightarrow U < s \cdot logN$ (Gessler 1995).

The second method is a stochastic Wright-Fisher simulation with selection, mutation and genetic drift (Figure 1B), in which: (i) individuals with a deleterious background can contribute to adaptation; (ii) a mutation-free population evolves towards a MSB without assuming a Poisson distribution of the number of deleterious alleles.

2.1. Wright-Fisher simulations

We track the number of individuals in each genotype class: ab/x, Ab/x, aB/x, and AB/x, where $x \geq 0$ is the number of deleterious alleles in non-specific loci. The simulations start with a single-peak smooth fitness landscape and a mutation-free population (all individuals start in the optimal $ab/0$ genotype with fitness 1) that accumulates

157 deleterious mutations over the first 5,000 generations of the simulation. With s=0.05
158 and 0.005, 180 and 1,800 generations are enough to get the average number of
159 deleterious alleles per individual to 99.99% of its MSB value, U/s (Gordo and
160 Dionisio 2005).

161 After 5,000 generations the fitness landscape changes to a rugged one, making *AB* the
162 optimal genotype with fitness $1+sH$ (Figure 1B). The simulation then proceeds until
163 an *AB* genotype appears and either fixates in the population or goes extinct (either all
164 or no individuals are in the *AB* classes, respectively). Therefore, each simulation
165 provides one sample of the waiting time for the appearance of a double mutant and
166 one sample of the probability of fixation of a double mutant. At least 1,000
167 simulations were performed for each parameter set.

168 Table 1 summarizes the model parameters with estimated values for *E. coli*.

169 3. Results

170 3.1. Appearance of a double mutant

171 We are interested in the waiting time for the appearance of a double mutant *AB*
172 either by a double mutation in a wildtype individual *ab*, or via a single mutation in a
173 single mutant *Ab* or *aB* (Figure 1A). Denoting the population size by N, we note that
174 (i) if $Ne^{-U/s}(\mu/s)^2 > 1$ then double mutants are already expected at the MSB and
175 adaptation will not require new mutations; (ii) if $Ne^{-U/s}\,\mu/s < 1$ then no single
176 mutants are expected at the MSB and double mutants must be generated by a double
177 mutation in a wildtype individual. In this case, increasing the mutation rate of

individuals with fitness below 1 will have no effect on the appearance of the double mutant and there is no point in analyzing the effect of SIM.

Combining the two constraints we get this constraint on the population size N: $e^{U/s}\, s/\mu < N < e^{U/s}(s/\mu)^2$. This constraint is reasonable for bacterial populations (see Table 1).

The frequencies of wildtype (*ab*) and single mutants (*aB* and *Ab* combined) that are mutation-free at the MSB are roughly $e^{-U/s}$ and $2\,\mu/s \cdot e^{-U/s}$, respectively. The probability that an offspring of a wildtype or single mutant parent is a double mutant *AB* is μ^2 and μ, respectively. The probability that such an offspring is also mutation-free in the rest of its genome (the only mutations that occurred were at the specific loci) is e^{-U}. Therefore, the probability q that a random offspring is a double mutant, given there are no double mutants in the current generation, is approximated by

$$q = \mu^2 e^{-\frac{U}{s}-U} + 2\frac{\mu^2}{s}e^{-\frac{U}{s}-U} \approx 2\frac{\mu^2}{s}\left(1-\frac{U}{s}\right). \quad (2)$$

The first expression assumes that individuals with a deleterious background don't contribute to adaptation and that the MSB distribution of deleterious alleles is Poisson. The second expression also assumes that mutation is much weaker than selection: $U \ll s$.

With SIM the mutation rate of single mutants is increased τ-fold and the probability that a random offspring is a double mutant is

$$q_{SIM} = \mu^2 e^{-\frac{U}{s}-U} + 2\frac{\tau\mu^2}{s}e^{-\frac{U}{s}-\tau U} \approx q \cdot \tau(1-\tau U). \quad (3)$$

These expressions use the same assumptions as in eq. 2. The second expression also assumes that $\tau U < 1$.

Appendix A includes full derivations of the above equations and Figure S1 compares them with simulations results.

3.2. Fixation probability of the double mutant

Assuming an advantage to the double mutant (H>1) and a large population size (see the above constraint on N), a double mutant has two possible fates after its appearance: fixation or extinction. Following Eshel (1981), the fixation probability ρ of the double mutant is (see Appendix B)

$$\rho \approx 2\frac{sH}{1+sH} \approx 2sH. \quad (4)$$

That is, the fixation probability of the double mutant is roughly twice its adaptive advantage. This is a classic result of population genetics theory (Fisher 1930, p. 76; Patwa and Wahl 2008).

The fixation probability with SIM equals that of NM and CM because the mutation rate of the wildtype *ab* equals that of the double mutant *AB* (but see an exception in section 3.5).

3.3. Adaptation rate

From the probability q that a random offspring is a double mutant, we can derive the probability that one or more double mutants appear in the next generation: $1 - (1-q)^N \approx Nq$. This is a good approximation because Nq is very small due to the constraint on N. Once a double mutant appears it goes to fixation with probability ρ.

When fixation is much faster than appearance of the double mutant *AB*, the time for adaptation *T* can be approximated by the waiting time for a double mutant that goes to fixation. This waiting time follows a geometric distribution with rate $Nq\rho$ and therefore the adaptation rate v (the inverse of the waiting time for adaptation) is approximately

$$v = E[T]^{-1} \approx Nq\rho. \tag{5}$$

Plugging eqs. 2-4 in eq. 5, we get these approximations:

$$v_{NM} = 2NH\mu^2 e^{-\frac{U}{s}-U}(2+s) \approx 4NH\mu^2\left(1-\frac{U}{s}\right) \tag{6}$$

$$v_{CM} = v_{NM}\cdot\tau^2 e^{\frac{-(\tau-1)U(1+s)}{s}} \approx v_{NM}\cdot\tau^2\left(1-\frac{\tau U}{s}\right) \tag{7}$$

$$v_{SIM} = v_{NM}\cdot\frac{2\tau e^{-(\tau-1)U}+s}{2+s} \approx v_{NM}\cdot\tau(1-\tau U) \tag{8}$$

NM is normal mutagenesis, CM is constitutive mutagenesis, and SIM is stress-induced mutagenesis. The middle expression in each equation is the full approximation, which assumes a Poison distribution and no contribution of deleterious genotypes to adaptation. The right hand sides are first order approximations that assume mutation is much weaker than selection ($U \ll s$ for NM and SIM, $\tau U \ll s$ for CM) and that $1<\tau<1/U$. See Table 1 for description of model parameters and an article by Weinreich and Chao (2005) for a result similar to eq. 6.

The main conclusions from eqs. 6-8: First, adaptation with CM is faster than with NM. Second, adaptation with SIM is also faster than with NM, but not as fast as with CM because the mutation-free wildtype (*ab/0*) does not hypermutate.

If mutation is weaker than selection ($U \ll s$) then the adaptation rate with CM increases with τ^2 and the adaptation rate with SIM increases with τ. In addition, because the fixation probability is the same for NM, CM and SIM, the differences in the adaptation rate are due to differences in the appearance probability q (Figure S1); see section 3.5 for a different scenario in which SIM also increases the fixation probability.

Figure 2 compares the analytic approximations with simulations results for the weak mutation regime ($U \ll s$). This regime is relevant for asexual microbes in which the deleterious mutation rate is generally 10^{-4}-10^{-3} mutations per genome per generation and selection coefficients are estimated to be between 10^{-1} and 10^{-2} (see Table 1). When the mutation rate fold increase τ is high (>10), the approximations slightly overestimate the adaptation rate because the double mutant *AB* is more likely to appear on a deleterious background (*AB*/*1* instead of *AB*/*0*). Because the fitness of *AB*/*1* is higher than that of the wildtype *ab*/*0* (this happens because $H>(1-s)^{-1}\approx 1+s$), the double mutant can go to fixation even when it appears on a deleterious background, sweeping the deleterious alleles with it to fixation in a process called "genetic hitch-hiking" (Maynard Smith and Haigh 1974). However, these sweeps result in a lower fixation probability for the double mutant (Figure S2).

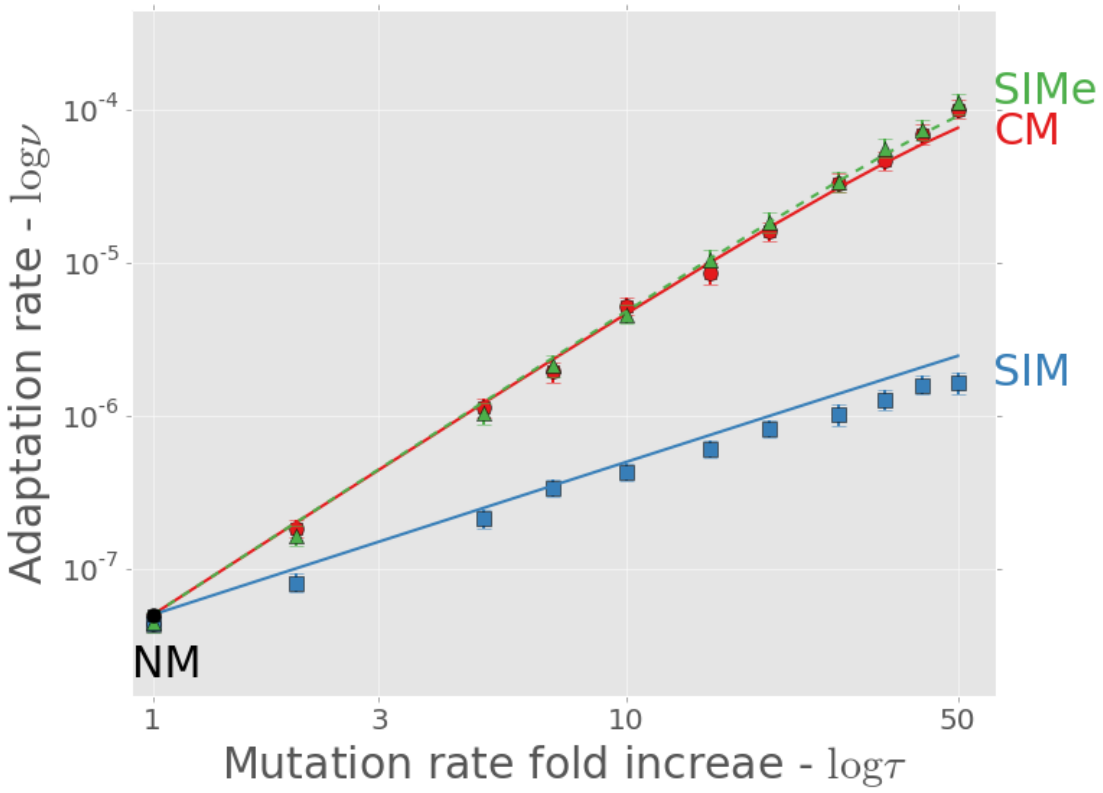

Figure 2 – Complex adaptation with different mutational strategies. The figure shows the adaptation rate ν as a function of the mutation rate increase τ (both in log scale). A black circle is normal mutagenesis (NM; τ=1); solid line with circles is constitutive mutagenesis (CM); solid line with squares is stress-induced mutagenesis (SIM); dashed lines with triangles is stress-induced mutagenesis with environmental stress (SIMe; see section 3.5). Lines are analytic approximations. Markers are the means of stochastic simulation results. Error bars represent 95% confidence interval of the mean (at least 1,000 simulations per point; computed with bootstrap with 1,000 samples per point). Parameters (see Table 1): U=0.0004, s=0.05, β=0.0002, H=2, N=10^6.

What happens when mutation is as strong as selection? Figure 3A shows results for s=10U. When the average number of deleterious alleles per individual $\tau U/s$ is over one, adaptation with CM is likely to occur on a deleterious background. Because our approximation neglects adaptation on deleterious backgrounds, it underestimates the adaptation rate (Figure 3A). Note that although the adaptation rate continues to increase with τ, the population carries more deleterious alleles after adaptation, resulting in a lower population mean fitness (Figure 3B) and eventually a lower fixation probability and adaptation rate (Figure 3A) .

With SIM, the average number of deleterious alleles per individual U/s does not increase with τ, because mutation-free individuals ($ab/0$) do not hypermutate. As in the case of weak mutation, when τ>10 the double mutant can appear on a deleterious background, resulting in hitch-hiking and a lower fixation probability, and causing our approximation to overestimate the adaptation rate (Figure 3A).

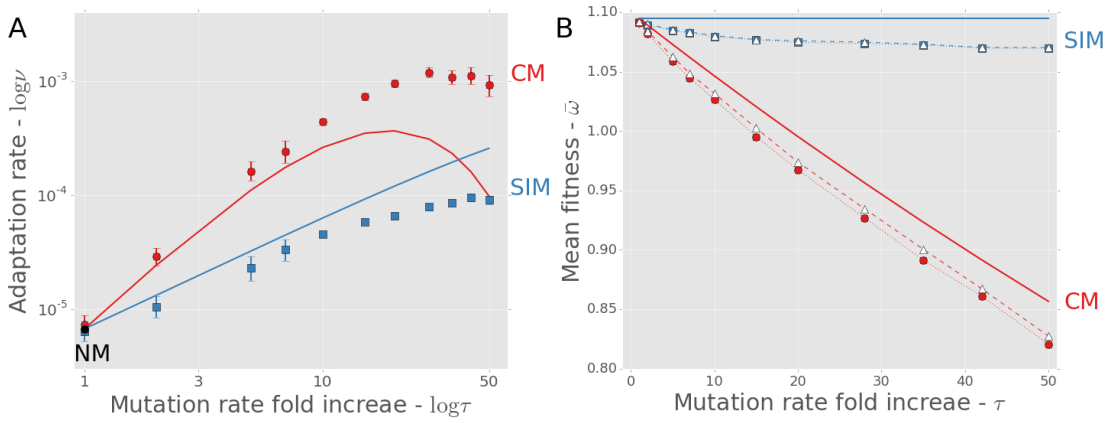

277

278 **Figure 3 – Adaptation with strong mutation.** When the deleterious mutation rate is high –
279 here U=s/*10* – the adaptation process can lead to hitch-hiking of deleterious alleles with the
280 beneficial double mutant. **(A)** The adaptation rate v as a function of the mutation rate increase
281 τ (both in log scale). A black circle for normal mutagenesis (NM; τ=1); red solid line and
282 circles for constitutive mutagenesis (CM); blue solid line and squares for stress-induced
283 mutagenesis (SIM). Lines are analytic approximations. Markers are the means of stochastic
284 simulations results. Error bars represent 95% confidence interval of the mean (at least 1,000
285 simulations per point; computed with bootstrap with 1,000 samples per point). Parameters
286 (see Table 1): U=0.005, s=0.05, β=0.0002, H=2, N=10^6. **(B)** The population mean fitness $\bar{\omega}$ after
287 successful fixation of the beneficial double mutant as a function of the mutation rate increase
288 τ. Solid lines are analytic approximations neglecting adaptation from deleterious background
289 ($e^{-\tau U}(1+sH)$); dotted lines with filled squares (SIM) and circles (CM) are the means of stochastic
290 simulation results; dashed lines with white triangles are predictions based on the genotype
291 on which *AB* appeared in the simulations, including MSB but disregarding the effects of drift
292 during the fixation process (which only has a significant effect with CM due to higher
293 mutation rates in the wildtype). Error bars are too small to see. Same parameter values as in
294 panel A.

295

3.4. The trade-off between *adaptability* and *adaptedness*

Next, we explore how different mutational strategies (NM, CM and SIM) balance between *adaptability* – the ability to adapt to new conditions – and *adaptedness* – the ability to remain adapted to current conditions. For this purpose we define *adaptedness* as $\bar{\omega}$ the population mean fitness in a stable environment and *adaptability* as *v the* rate of complex adaptation.

We used the above approximations (eqs. 6-8) to calculate the adaptation rate of populations with NM, CM and SIM. We also extended an existing model (Ram and Hadany 2012) to calculate the population mean fitness at the mutation-selection balance. This extended model includes beneficial mutations and allows more than one mutation to occur in the same individual and generation. The details of this model and the calculation of population mean fitness with various mutational strategies are given in Online Appendix D.

The mutation rate with CM is constant and uniform across the population, and the population mean fitness mainly depends on the fitness and mutation rate of the fittest individuals. Therefore, the population mean fitness decreases when the mutation rate increases; this decrease is due to generation of deleterious mutations in the fittest individuals. The adaptation rate, however, increases with the mutation rate (eq. 7). This trade-off between *adaptability* and *adaptedness* constraints the population: after a long period of environmental stability it can lose the potential for adaptation, and after a long period of environmental change the population can be susceptible to reduced fitness and mutational meltdowns (Lynch et al. 1993).

318 However, this trade-off between *adaptability* and *adaptedness* can be broken if
319 mutation rates are not uniform across the population. Increased mutation rates in
320 unfit individuals increase the population mean fitness, as long as beneficial (or
321 compensatory) mutations can occur (Ram and Hadany 2012). Figure D1 shows this
322 advantage of SIM over NM in terms of the difference in population mean fitness
323 ($\bar{\omega}_{SIM} - \bar{\omega}_{NM}$). Moreover, increased mutation rates in unfit individuals also increase
324 the adaptation rate (eq. 8; Figure 2). Therefore, SIM breaks the trade-off between
325 *adaptability* and *adaptedness*.

326

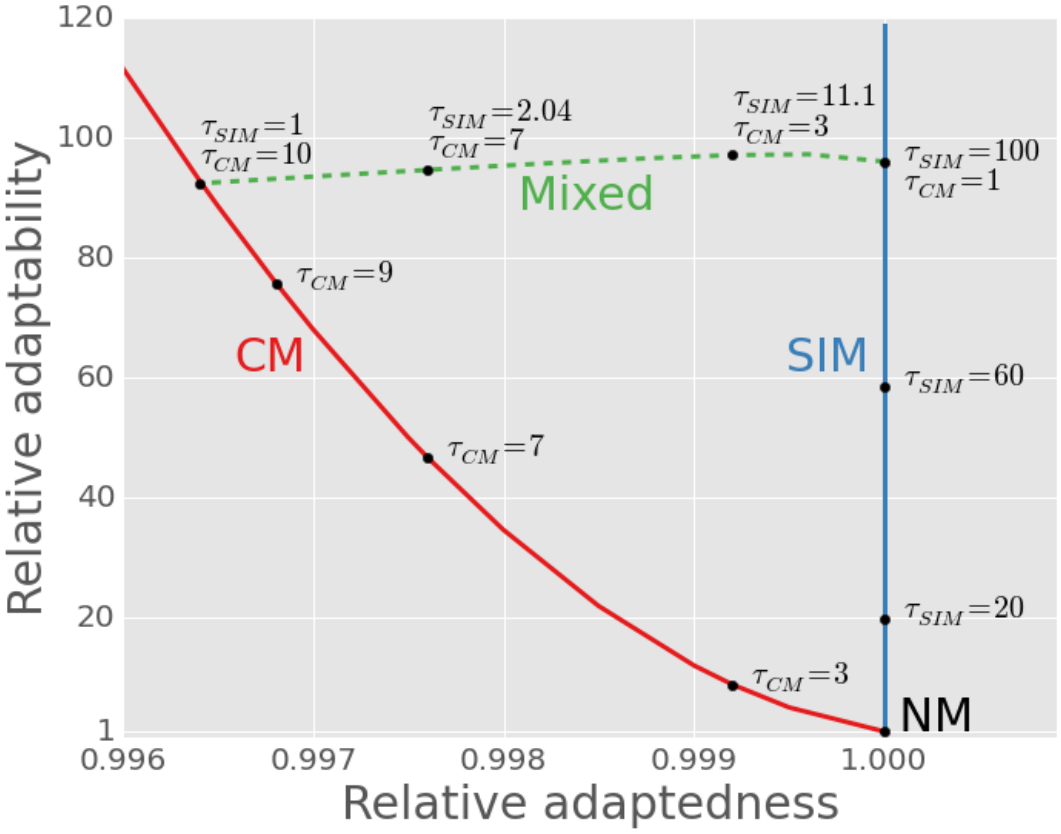

Figure 4 – The trade-off between *adaptedness* and *adaptability*. The figure shows the relative *adaptedness* and the relative *adaptability* of different mutational strategies in comparison to normal mutagenesis (NM). *Adaptedness* is defined by the population mean fitness at MSB, $\bar{\omega}$ (see Online Appendix D). *Adaptability* is defined by the rate of complex adaptation, ν (eqs. 6-8). Constitutive mutagenesis (CM) increases the mutation rate of all individuals τ_{CM}-fold; Stress-induced mutagenesis (SIM) increases the mutation rate of stressed individuals τ_{SIM}-fold; Mixed strategies (dashed line) increase the mutation rate of all individuals τ_{CM}-fold and of stressed individuals an additional τ_{SIM}-fold. SIM breaks off the *adaptability-adaptedness* trade-off of CM, increasing the *adaptability* without compromising the *adaptedness* of the population. Parameters (see Table 1): N=10^6, U=0.0004, β=0.0002, s=0.05, H=2, τ<<s/U.

Figure 4 shows the adaptation rate and population mean fitness of CM and SIM compared to NM for different values of τ, the mutation rate fold increase.

Any realistic rate of adaptation v can be realized using both CM and SIM. The highest mean fitness will always be attained with SIM, which has a small advantage over NM (that cannot be seen in this figure, but see Figure D1) due to the increased generation of beneficial mutations in individuals with low fitness. If for some rate of adaptation the mutation rate fold increase τ required by SIM is too high (*i.e.*, $\tau U > s$), the same adaptation rate can be realized by a mixed strategy (dashed line in Figure 4). For example, a 96-fold increase in adaptation rate can be achieved with CM with τ=10, with SIM with τ=96, or with a mixed strategy with τ_{CM}=7 and τ_{SIM}=2 in which all individuals increase their mutation rate 7-fold and stressed individuals further increase their mutation rate 2-fold. However, these increases in adaptation rates have a price: the mutational load will decrease the population mean fitness from 0.9996 with NM to 0.996 with CM and 0.9972 with the mixed strategy. This price in not paid by populations with SIM because the mean fitness mainly depends on the mutation rate of fit individuals.

3.5. Environmental stress

So far, we considered the case where the environmental change creates an opportunity for adaptation without affecting the absolute fitness of the population – for example, a new ecological niche can be favorable without affecting the well-being of the current population. In that scenario, the wildtype *ab* was not stressed and did not hypermutate.

Next, we consider a different scenario in which an environmental change affects the well-being of the entire population: for example, exposure to an antibiotic drug or a host immune response. In this case the environmental change doesn't just create an opportunity for adaptation but also causes stress in the entire population. We use a subscript *e* to denote quantities related with this scenario.

As before the double mutant *AB* is resistant to the stress (*i.e.* the drug or immune response) and therefore has a higher fitness than either the wildtype or the non-resistant single mutants. However, in this scenario the wildtype *ab* is also stressed and therefore hypermutates with SIM (compare with eq. 1):

$$U_e(\omega) = \begin{cases} U, & \omega > 1 \\ \tau U, & \omega \leq 1 \end{cases}. \tag{9}$$

This scenario has an important biological relevance, as SIM has been implicated in the evolution of drug resistance in bacteria and yeast (Cirz and Romesberg 2007; Obolski and Hadany 2012; Shor et al. 2013) and could be involved in the evolution of pathogen virulence and the evolution of drug resistance and progression in cancer cells.

We assume that after the environmental change the SIM_e population has reached a new MSB (Gordo and Dionisio 2005) with mutation rate τU, before the appearance of the double mutant (with s=0.05 and U=0.0004, for example, the average number of deleterious mutations is $0.99 \cdot U/s$ after 90 generations, whereas the adaptation time is well over 1,000 generations). Under this assumption, the adaptation rate with SIM_e is (see Appendix C for full derivation)

$$v_{SIM_e} \approx v_{CM} \cdot \left(1 + \frac{U(\tau-1)}{sH}\right). \quad (10)$$

That is, adaptation with SIM_e is faster than with CM (Figure 2A). The fixation probability of double mutants is higher with SIM_e than with CM, because the mutation rate of double mutants is lower than that of the rest of the population. This difference in mutation rates confers an additional selective advantage to the double mutants (see Appendix C) which increases their fixation probability:

$$\rho_{SIM_e} \approx \rho \left(1 + \frac{U(\tau-1)}{sH}\right). \quad (11)$$

This additive advantage increases linearly with τ with a slope of U/sH and can be significant: for s=0.05, H=2 and U=0.0004, increasing the mutation rate of stressed individuals 10-fold increases the fixation probability by 3.6%. The increased fixation probability was verified by simulations (Figure S2).

4. Discussion

We studied the effect of stress-induced mutagenesis (SIM) on both the *adaptability* – the capacity of populations to adapt to new conditions – and the *adaptedness* – the ability of populations to stay adapted to existing conditions (Leigh 1970). We showed that SIM breaks the trade-off between *adaptability* and *adaptedness*, allowing rapid adaptation to complex environmental challenges without compromising the population mean fitness in a stable environment.

In addition to the pure strategies of constitutive mutagenesis (CM) and SIM, our model also considers a mixed mutational strategy. There are two examples of such a mixed strategy. First, if individuals have incomplete information regarding their

condition (this is the case in most realistic biological scenarios) then we expect errors in the induction of mutagenesis: induction of mutagenesis without stress and failure to induce mutagenesis under stress. In this case the population would, on average, use a mixed strategy. Second, a mutator allele can increase the mutation rate constitutively and further increase it under stress – for example, a recent study with *Pseudomonas aeruginosa* found that although the *mutS*, *mutY* and *mutM* mutator alleles always increase the mutation rate in comparison with the wildtype, the level of this increase depends on the level of stress the cell experiences (Torres-Barceló et al. 2013).

Our model does not assume direct fitness costs for any of the mutational strategies. A "cost of DNA replication fidelity" (Dawson 1998) – the energy and time expended in order to maintain a low mutation rate – could make both CM and SIM more successful. The "cost of fidelity" may require further study, but empirical evidence suggests that it doesn't play an important role in the evolution of the mutation rate (Giraud et al. 2001a; Loh et al. 2010; Gentile et al. 2011; Shee et al. 2011). Another fitness cost might be associated with the regulation of the mutation rate: for individuals to determine if their condition calls for the induction of mutagenesis, they must invest resources and energy in costly sensory mechanisms. However, such mechanisms already exist for various unrelated purposes, such as the maintenance of cell cycle and homeostasis. Therefore, we consider these mechanisms as "free" in terms of fitness costs. Moreover, in *E. coli* mutagenesis is induced by several stress responses that serve other cellular functions (Foster 2007; Al Mamun et al. 2012), and this is probably the case in other organisms as well.

Our model focuses on asexual populations, ignoring recombination, segregation, and sexual reproduction. These mechanisms are important for adaptation on a rugged fitness landscape both because they help to cope with deleterious mutations and because they allow different single mutants to produce double mutants without an increased mutation rate. We expect that recombination will reduce the advantage of SIM over NM in terms of population mean fitness (Agrawal 2002), direct competitions (Tenaillon et al. 2000), and adaptation rate (due to the Fisher-Muller effect).

Mean fitness and adaptation rate are both population-level traits. But simply because SIM has the most efficient balance between these traits doesn't mean it will necessarily evolve, because individual-level selection and population-level selection can act in opposing directions. In a previous article we have demonstrated that 2nd order selection can lead to the evolution of SIM (Ram and Hadany 2012): in an asexual population evolving on a smooth fitness landscape, selection favored SIM over both NM and CM. In the current article we show that selection also favors SIM on a rugged fitness landscape (Online Appendix F).

Complex traits, coded by multiple genes, present an open evolutionary problem, first described by Sewall Wright in 1931: if different alleles are separately deleterious but jointly advantageous, how can a population evolve from one co-adapted gene complex to a fitter one, crossing a less fit "valley"? Wright suggested the "shifting-balance theory of evolution" (Wright 1931; Wright 1988). His solution is valid (Crow et al. 1990; Wade and Goodnight 1991; Peck et al. 2000) but possibly limited to specific parameter ranges (Moore and Tonsor 1994; Gavrilets 1996; Coyne et al. 2000;

Whitlock and Phillips 2000). As a result, other mechanisms have been proposed: increased phenotypic variance after population bottlenecks (Whitlock 1995); environmental fluctuations (Whitlock 1997); environmental heterogeneity (Hadany 2003); fitness-associated recombination (Hadany and Beker 2003); and intermediate recombination rates (Weissman et al. 2010). Our model of complex adaptation is similar to that of Weinreich and Chao (2005), but our model includes various mutational strategies and the effects of stress and deleterious mutations. Our results (Figure 2) suggest that SIM can help resolve the problem of fitness valley crossing by reducing the time required for a population to shift an adaptive peak.

Our results provide theoretical basis to the conjecture that SIM facilitates adaptation. This conjecture can be tested experimentally, for example, with *E. coli*, where it is possible to interfere with the regulation of mutagenesis (Cirz and Romesberg 2007). The adaptation time with and without SIM can be measured in an experimental population adapting on a two-peak fitness landscape (Schrag et al. 1997). These measurements can then be compared to our analytic approximations to determine the relative advantage and disadvantage of the different mutational strategies.

Conclusions

Stress-induced mutagenesis has been implicated as a driver of adaptive evolution for several decades (Cairns et al. 1988; Tenaillon et al. 2004; Rosenberg et al. 2012). We provide theoretical treatment of this concept. Our results show that stress-induced mutagenesis increases the rate of complex adaptation, and that in contrast to constitutive mutagenesis it does not jeopardize the fitness of populations under stable conditions. Because mutation is a fundamental force in every biological

system, these results have important implications on many fields in the medical and life sciences, including epidemiology, oncology, ecology, and evolutionary biology.

5. Acknowledgments

We thank Uri Obolski for advice on statistical analysis. We are grateful to A.F. Agrawal for helpful comments on an earlier version of the manuscript. This research has been supported in part by the Israeli Science Foundation 1568/13 (LH) and by Marie Curie reintegration grant 2007–224866 (LH).

6. Appendixes

Appendix A: Appearance of a double mutant

In the following analysis we assume that $0 < \mu \ll U \ll s \ll 1$ and $s/\mu < N < (s/\mu)^2$ – see model overview for details. This also means that $U + 2\mu \approx U$ and $U/s + U \approx U/s$. The probability q that a random offspring in the next generation is AB given there are no AB in the current generation can be approximated by:

$$q = \mu^2 e^{-\frac{U}{s}-U} + 2\frac{\mu^2}{s}e^{-\frac{U}{s}-U} = \frac{\mu^2}{s}e^{-U-\frac{U}{s}}(s+2) \approx \frac{\mu^2}{s}\left(1-U-\frac{U}{s}\right)(2+s).$$

Using the above assumptions, this resolves to:

$$q \approx 2\frac{\mu^2}{s}\left(1-\frac{U}{s}\right).$$

Taking the derivative with respect to U and denoting $g = U/\mu$ (g can be thought of as the number of non-specific loci in the genome):

$$\frac{dq}{dU} = \frac{2U(2s-3U)}{g^2 s^2} > 0 \Leftrightarrow U < \frac{2}{3}s.$$

So q increases with U because the right hand side is guaranteed to be true under the assumption $U \ll s$.

For a population with SIM

$$q_{SIM} = \mu^2 e^{-\frac{U}{s}-U} + 2\frac{\tau\mu^2}{s}e^{-\frac{U}{s}-\tau U} \approx \frac{\mu^2}{s}\left(1-\frac{U}{s}\right)\left(s(1-U)+2\tau(1-\tau U)\right) = \frac{\mu^2}{s}\Big(1-\frac{U}{s}\Big)\left(s(1-U)+2\tau(1-U)-2\tau(\tau-1)U\right) = \frac{\mu^2}{s}\left(1-\frac{U}{s}\right)\left((s+2\tau)(1-U)-2\tau(\tau-1)U\right) \approx \frac{\mu^2}{s}\left(1-\frac{U}{s}\right)(2\tau(1-U)-2\tau(\tau-1)U).$$

The last approximation assumes that $\tau \geq 1 \Rightarrow s \ll 2\tau$. Rearranging the last result, we find the approximation

$$q_{SIM} \approx 2\tau\frac{\mu^2}{s}\left(1-\frac{U}{s}\right)(1-\tau U) = \tau(1-\tau U)q.$$

Taking the derivative with respect to τ,

$$\frac{dq_{SIM}}{d\tau} = q(1-2\tau U) > 0 \Leftrightarrow \tau U < \frac{1}{2},$$

because q, U, and τ are all positive. So the condition $\tau U \ll s \ll 1$ guarantees that q_{SIM} increases with τ, and it is also sufficient for $q_{SIM} > q$ (not shown).

Appendix B: Fixation of a double mutant

Following Eshel (1981), the fixation probability ρ of the double mutant AB is

$$\rho = 2\frac{\alpha-1}{\alpha} + o(\alpha-1),$$

where α is the fitness of the double mutant relative to the population mean fitness $\bar{\omega}$ and assuming that fitness is measured by the average number of progeny which is Poisson distributed:

$$\alpha = \frac{(1+sH)e^{-U}}{\bar{\omega}}.$$

Here, we only consider progeny without new deleterious mutations; their fraction is e^{-U}. This factor cannot be ignored because there is variation in mutation rates within the population (see "minor technical point" by Johnson and Barton (Johnson and Barton 2002)). At this stage, double mutants are still very rare, so we can use the population mean fitness at the MSB. The population mean fitness can be approximated by $\bar{\omega} = e^{-U}$ (see *supporting information*). Therefore,

$$\rho = 2\frac{sH}{1+sH} + o(sH).$$

Assuming sH is small ($sH \ll 1$) we can approximate this by

$$\rho \approx 2sH.$$

Appendix C: Fixation of a double mutant with SIMe

With SIMe the mutation rate of *ab* is τU while that of *AB* is only U. We assume the population reached a MSB before the fixation of *AB* because convergence to MSB (Gordo and Dionisio 2005) is much faster than adaptation. Following the derivation in Appendix 2, the relative fitness of SIMe is

$$\alpha_{SIMe} = \frac{(1+sH)e^{-U}}{e^{-\tau U}} = (1+sH)e^{U(\tau-1)}.$$

Plugging that in the fixation probability,

$$\rho_{SIM_e} \approx 2\frac{(1+sH)e^{U(\tau-1)}-1}{(1+sH)e^{U(\tau-1)}} = 2\frac{1+sH-e^{-U(\tau-1)}}{1+sH} = \rho + 2\frac{1-e^{-U(\tau-1)}}{1+sH}.$$

This can be simplified by a 1st order approximation for $e^{-U(\tau-1)}$:

525 $$\rho_{SIM_e} \approx \rho + 2\frac{U(\tau-1)}{1+sH} = \rho\left(1+\frac{U(\tau-1)}{sH}\right).$$

526 Because $\frac{U(\tau-1)}{sH} > 0$, the right hand side is greater than 1. Therefore,

527 $$\rho_{SIM_e} > \rho.$$

528 Because the appearance with SIM$_e$ is the same as with CM, the adaptation rate with

529 SIM$_e$ can be written as

530 $$\nu_{SIM_e} = Nq\rho_{SIM_e} = Nq\rho\left(1+\frac{U(\tau-1)}{sH}\right) = \nu_{CM}\cdot\left(1+\frac{U(\tau-1)}{sH}\right).$$

531 Online Appendix D: Mean fitness at the mutation-selection

532 balance

533 Denote the frequency of individuals with x deleterious alleles by f_x. The frequency of

534 such individuals in the next generation f'_x is given by

$$\bar{\omega} f'_x = \sum_{y\geq 0} f_y m_{x,y},$$

535 where $m_{x,y}$ is the transition probability from y deleterious alleles to x deleterious

536 alleles and $\bar{\omega}$ is the population mean fitness.

537 The term $m_{x,y}$ consist of the fitness of individuals with y deleterious alleles, ω_y, and

538 the probability that the precise number of mutations occurred. Specifically, if $y \geq x$

539 then exactly y-x beneficial mutation must occur; if $y \leq x$ then exactly x-y deleterious

540 mutations must occur:

541 $$m_{x,y} = \begin{cases} \omega_y \cdot P(x-y\ deleterious\ mutations), & y < x \\ \omega_y \cdot P(y-x\ beneficial\ mutations), & y > x \\ \omega_y \cdot P(no\ mutations), & y = x \end{cases}.$$

Using the probability mass function of a Poisson distribution, we can expand the above equation to

$$\bar{\omega} f_x' = \sum_{y \le x} f_y \omega_y \frac{e^{-\delta U_y} (\delta U_y)^{x-y}}{(x-y)!} + \sum_{y \ge x} f_y \omega_y \frac{e^{-\beta U_y} (\beta U_y)^{y-x}}{(y-x)!}, \quad \forall x \ge 0,$$

where ω_y is the fitness of individuals with y deleterious alleles, $\bar{\omega}$ is the population mean fitness ($\bar{\omega} = \sum \omega_x f_x$), δ and β are the fraction of mutations that are deleterious and beneficial, respectively ($\delta+\beta=1$ and $0 \le \beta < \delta \le 1$), and U_y is the average number of new mutations per generation in an individual with y deleterious alleles.

This can be written as a matrix equation by multiplying the frequencies vector f and the mutation-selection matrix M:

$$\bar{\omega} f' = M f$$

At the mutation-selection balance (MSB), f^* solves the equation (a star * denotes equilibrium quantities)

$$\bar{\omega}^* f^* = M f^*.$$

Without beneficial mutations ($\delta=1$ and $\beta=0$), the above equation simplifies to

$$\bar{\omega} f_x' = \sum_{y \le x} f_y \omega_y \frac{e^{-U_y} {U_k}^{x-y}}{(x-y)!}, \quad \forall x \ge 0$$

and M is a triangular matrix. In this case the population mean fitness can be found by solving the equation for f_0:

$$\bar{\omega} f_0 = f_0 m_{0,0} = f_0 \omega_0 e^{-U_0} \Rightarrow \bar{\omega} = \omega_0 e^{-U_0},$$

558 which means that the population mean fitness is equal to the product of the fitness of
559 mutation-free individuals and the probability that a mutation-free individual does
560 not mutate. If $\omega_x = (1-s)^x$ and $U_x = U$ (constant uniform mutation rate) then
561 $\bar{\omega} = e^{-U}$ (Kimura and Maruyama 1966) and by the forward substitution method the
562 frequencies vector is

563 $$f_x = e^{-U/s}\,(U/s)^x/x!,$$

564 that is, the number of deleterious mutations per individual is Poisson distributed
565 with average U/s (Haigh 1978). With constitutive mutagenesis (CM), the population
566 mean fitness at the MSB is $e^{-\tau U}$: it decays exponentially as a function of τ the
567 mutation rate fold increase. In contrast, stress-induced mutagenesis (SIM), as shown
568 by Agrawal (2002), does not change the population mean fitness with respect to
569 normal mutagenesis (NM). This is because the least loaded individuals (x=0), with
570 fitness ω_0=1, also have the lowest mutation rate, U, and therefore the population
571 mean fitness is e^{-U}.

572 With beneficial mutations (β>0), the matrix M is a positive matrix, and by the *Perron-*
573 *Frobenius Theorem* (Otto and Day 2007, p. 709) $\bar{\omega}^*$ is the largest eigenvalue of M and f^*
574 is its unique positive eigenvector with $\sum f = 1$.

575 This eigenvalue problem is hard to solve analytically, however, by neglecting
576 elements outside the main three diagonals of M we have shown before (Ram and
577 Hadany 2012) that the population mean fitness increases with the mutation rate of
578 individuals with a below–average fitness:

579 $$sign\frac{\partial\bar{\omega}}{\partial U_x} = sign(\bar{\omega} - \omega_x).$$

Nevertheless, this framework allows the numerical calculation of the population mean fitness for finite n-by-n mutation-selection matrices by defining n such that $\omega_x = 0 \; \forall x \geq n$. The mean fitness of populations with different mutational strategies is then calculated by manipulating U_x.

Figure C1 shows that e^{-U} is a good approximation to the population mean fitness (because $\beta \ll \delta < 1$), and that SIM slightly increases the population mean fitness with respect to NM; a sufficient condition is that the mutation rate of individuals with below average fitness is increased (Ram and Hadany 2012). Since we assume that $U < s$, then $e^{-U} \approx 1 - U > 1 - s$. Therefore, for SIM to increase the population mean fitness it must increase the mutation rate in individuals with at least one deleterious mutation.

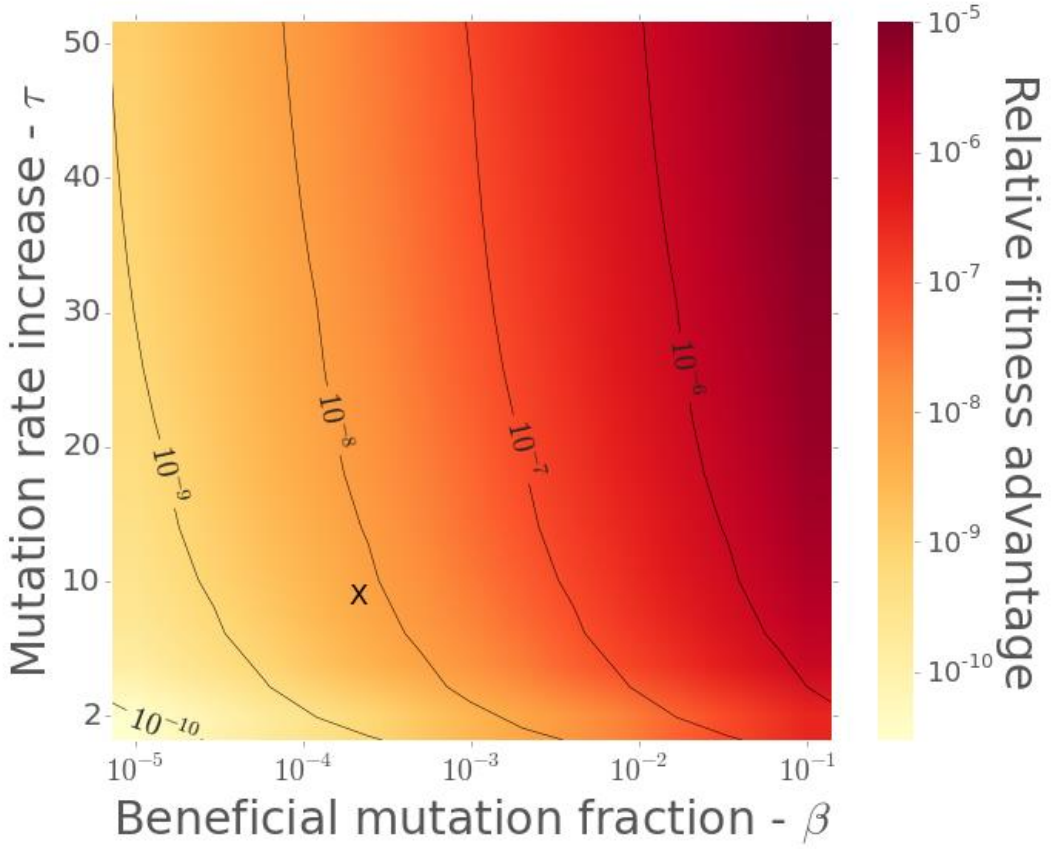

592

593 **Online Figure C1 – Mean fitness at the mutation-selection balance with stress-induced**

594 **mutagenesis.** The brightness represents the fitness advantage of stress-induced mutagenesis

595 over normal mutagenesis $((\bar{\omega}_{SIM} - \bar{\omega}_{NM})/\bar{\omega}_{NM})$ at the mutation-selection balance. The x-axis

596 is the fraction of mutations that are beneficial β. The y-axis is the mutation rate fold increase

597 under stress τ. "X" marks the parameter set β=1/5000 and τ=10, in which the fitness advantage

598 of SIM is ~$5 \cdot 10^{-9}$.

599

Online Appendix E: Possible relationships between stress and mutation

In the main text we used a threshold relationship between stress and mutation: if fitness drops below a threshold (<1 for SIM, ≤1 for SIM_e), the mutation rate increases τ-fold. But the relationship between stress and mutation can be more complex. For example, Agrawal (2002) has used a continuous relationship defined by a curvature parameter k. This relationship defines the mutation rate for an individual with fitness ω, baseline mutation rate U, and a maximal mutation rate fold increase τ as

$$U(\omega) = \tau U - (\tau - 1) U \omega^k.$$

When k approaches 0 this expression approaches U, corresponding to the NM strategy. When k approaches infinity this expression approaches eq. 1(1), corresponding to the SIM threshold strategy. See Figure E1 for a plot of these continuous relationships for various values of k.

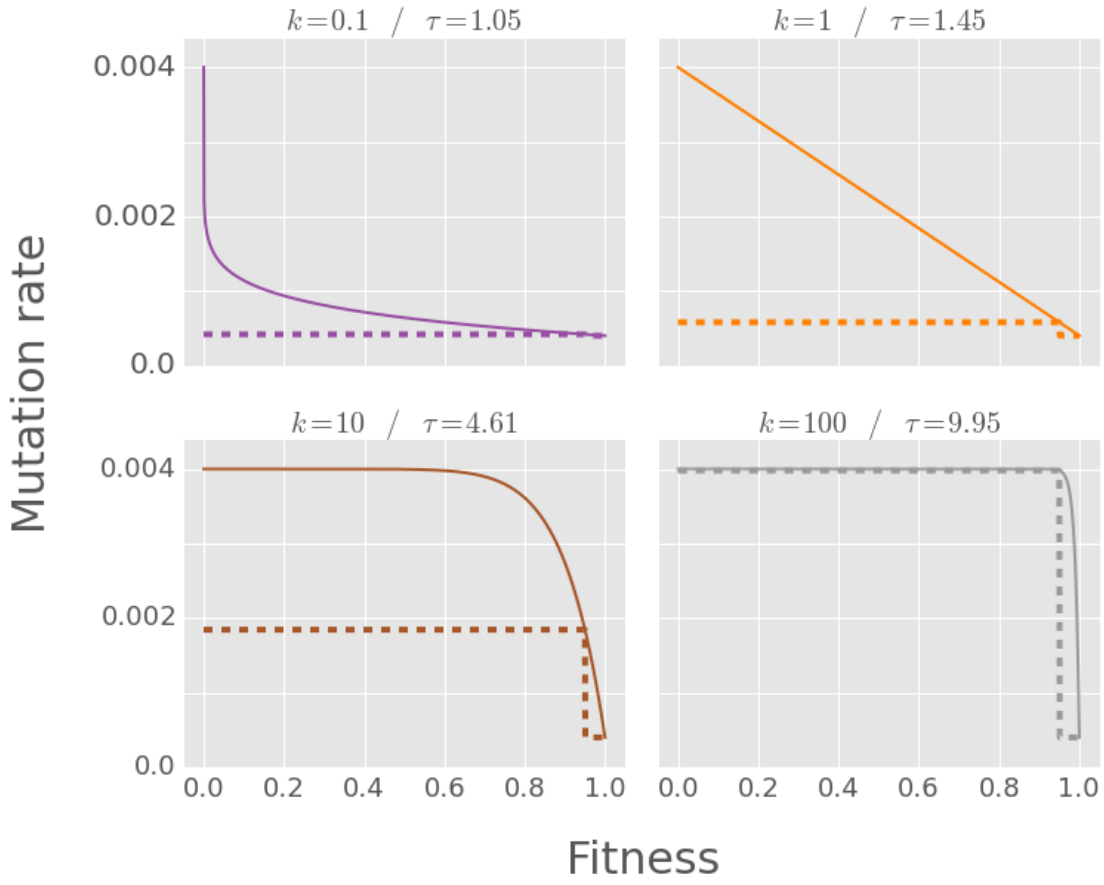

Online Figure E1– Different relationships between stress and mutation. The figure shows continuous relationships between fitness (x-axis) and mutation rate (y-axis) in solid lines and threshold relationships in dashed lines. The threshold relationship is defined in section 2 of the main text. The continuous relationships are defined in Supporting Text S4. Each panel shows a pair of relationships, with k increasing from 1/10 (convex relationship), to 1 (linear relationship) to 10 and 100 (concave relationships). Each continuous relationship is compared with a threshold relationship that has the same mutation rate for wildtypes (*ab/0*) and single mutants (*Ab/0*, *aB/0*, *ab/1*). Figure S5 shows that the adaptation rate with such threshold relationship approximates the adaptation rate with a continuous relationship.

Figure E2 shows the adaptation time for three continuous strategies (k=1/10, 1, and 10). Remarkably, the dynamics of a continuous strategy can be approximated by a threshold strategy by matching the mutation rates of single mutants:

$$U(\omega) = \begin{cases} U, & \omega \geq 1 \\ \tau U - (\tau - 1)U(1 - s)^k, & \omega < 1 \end{cases}.$$

This is equivalent to using a threshold strategy with mutation rate increase τ-(τ-1)(1-s)^k. The dashed lines in Figure E2 demonstrate this approximation. The continuous strategies can be approximated by threshold strategies because the main factor determining the adaptation rate is the mutation rate increase of the wildtype and the single mutants (*ab*, *aB*, and *Ab*). This is because individuals with more than a single mutation do not have a significant contribution to adaptation.

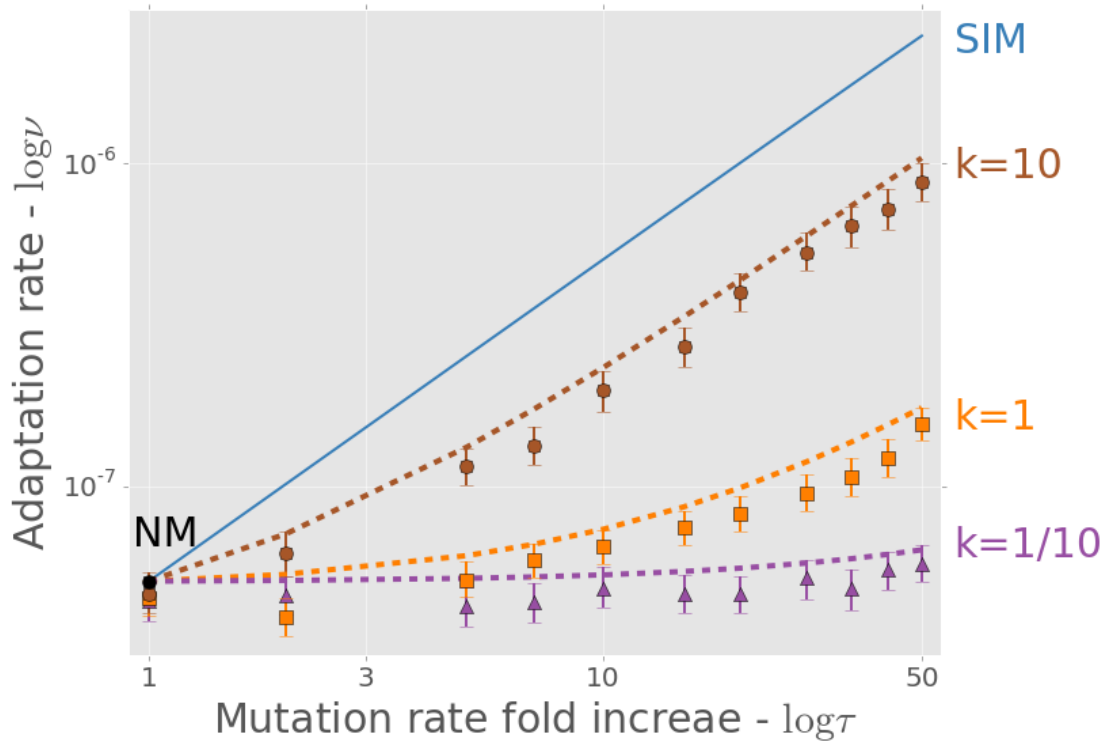

635

636 **Online Figure E2 – Complex adaptation with continuous relationship stress-induced**
637 **mutagenesis.** The figure shows the adaptation rate ν as a function of the mutation rate
638 increase τ (both in log scale). The solid line is an analytical approximation of SIM (same as in
639 Figure 2). Markers are the results of simulations of adaptation with SIM with different
640 continuous relationships between fitness and mutation rate. These continuous relationships
641 are defined by a mutation rate fold increase τ=10 and a curvature parameter k=10, 1, and 1/10,
642 top to bottom (see Supporting Text S4 and Figure S3 for more details on continuous SIM).
643 Each dashed line is an approximation of a continuous SIM using a SIM threshold strategy (eq.
644 13Error! Reference source not found.) with τ=4.61, 1.45, and 1.05, top to bottom. The fit
645 between the dashed lines and the corresponding markers suggests that a threshold strategy
646 captures the adaptive dynamics. Error bars represent 95% confidence interval of the mean (at
647 least 1,000 simulations per point; computed with bootstrap with 1,000 samples per point).
648 Parameters (see Table 1): U=0.0004, s=0.05, β=0.0002, H=2, N=10^6.

649

650 # Online Appendix F: Competitions between mutational strategies

651 We also simulated direct competitions between the different mutational strategies
652 (NM, CM, and SIM). In these competitions, half of the population alters its
653 mutational strategy to an invading strategy at the time of the environmental change.
654 Each simulation provides a sample of the frequency of the invading strategy after the
655 appearance and subsequent fixation or extinction of the double mutant *AB*. If the
656 average final frequency is significantly lower or higher than 50% we consider the
657 invading strategy disfavored or favored by natural selection over the initial strategy.
658 Statistical significance was calculated using a 1-sample 2-tailed t-test.

659 Figure F1 summarizes the competitions. CM clearly loses to both SIM and NM (first
660 and second panels from the right). SIM is significantly advantageous over NM when
661 the mutation rate increase is large enough (τ>2; 2-tail t-test, P<0.0015).

662 These results show that the evolutionary advantage of SIM at the population-level
663 corresponds to an individual-level advantage and can lead to the evolution of stress-
664 induced mutagenesis by natural selection, even when constitutive mutagenesis is
665 strongly disfavored. This is consistent with previous results in smooth fitness
666 landscapes (Ram and Hadany 2012).

667

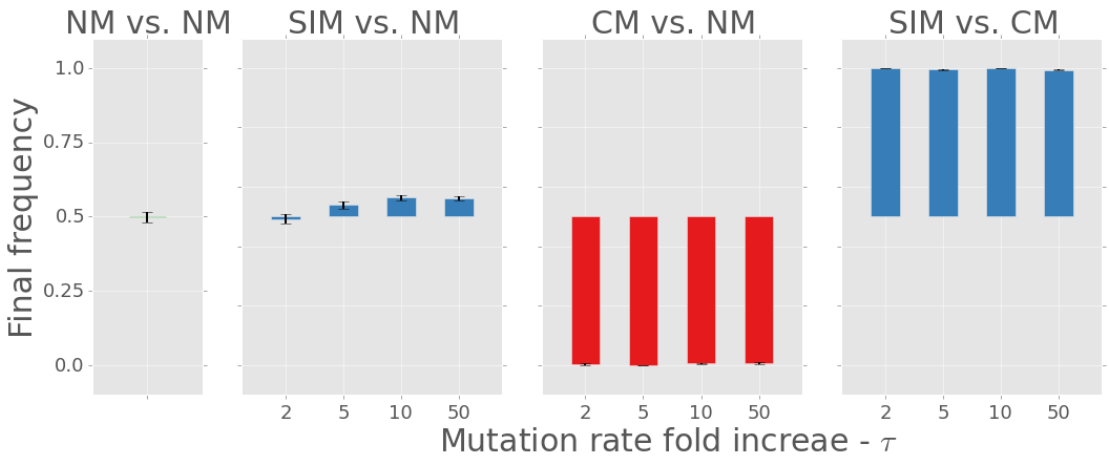

668

669 **Online Figure F1 – Direct competitions between three mutational strategies.** The figure
670 shows the average final frequency of (from right to left): stress-induced mutagenesis (SIM) vs.
671 constitutive mutagenesis (CM); CM vs. normal mutagenesis (NM); SIM vs. NM; and NM vs.
672 NM (control). Initial frequencies are always 0.5. Several mutation rate fold increases are
673 shown on the x-axis. SIM defeats CM and is significantly advantageous over NM when $\tau>2$
674 (2-tail t-test, $P<0.0015$). CM losses to NM and SIM ($P\approx0$). Therefore, SIM is favored by
675 selection over both NM and CM. Changing roles between resident and invader didn't affect
676 the results (not shown). Error bars represent the standard error of the mean (500 simulations
677 per point). Parameters (see Table 1): $U=0.0004$, $s=0.05$, $\beta=0.0002$, $H=2$, $N=106$.

678

7. Literature cited

Agrawal, A. F. 2002. Genetic loads under fitness-dependent mutation rates. Journal of Evolutionary Biology 15:1004–1010.

Al Mamun, A. A. M., M.-J. Lombardo, C. Shee, A. M. Lisewski, C. Gonzalez, D. Lin, R. B. Nehring, et al. 2012. Identity and function of a large gene network underlying mutagenic repair of DNA breaks. Science 338:1344–8.

Baharoglu, Z., and D. Mazel. 2011. *Vibrio cholerae* triggers SOS and mutagenesis in response to a wide range of antibiotics: a route towards multiresistance. Antimicrobial agents and chemotherapy 55:2438–41.

Berg, O. G. 1996. Selection intensity for codon bias and the effective population size of *Escherichia coli*. Genetics 142:1379–82.

Bjedov, I., O. Tenaillon, B. Gérard, V. Souza, E. Denamur, M. Radman, F. Taddei, et al. 2003. Stress-induced mutagenesis in bacteria. Science 300:1404–9.

Bristow, R. G., and R. P. Hill. 2008. Hypoxia and metabolism: Hypoxia, DNA repair and genetic instability. Nature reviews. Cancer 8:180–92.

Cairns, J., J. Overbaugh, and S. Miller. 1988. The origin of mutants. Nature 335:142–5.

Cirz, R. T., and F. E. Romesberg. 2007. Controlling mutation: intervening in evolution as a therapeutic strategy. Critical reviews in biochemistry and molecular biology 42:341–54.

Coyne, J. A., N. H. Barton, and M. Turelli. 2000. Is Wright's shifting balance process important in evolution? Evolution 54:306–317.

Crow, J. F., W. R. Engels, and C. Denniston. 1990. Phase Three of Wright's Shifting-Balance Theory. Evolution 44:233.

Dawson, K. J. 1998. Evolutionarily stable mutation rates. Journal of theoretical biology 194:143–57.

De Visser, J. A. G. M. 2002. The fate of microbial mutators. Microbiology (Reading, England) 148:1247–52.

Debora, B. N., L. E. Vidales, R. Ramírez, M. Ramírez, E. A. Robleto, R. E. Yasbin, and M. Pedraza-Reyes. 2010. Mismatch Repair Modulation of MutY Activity Drives *Bacillus subtilis* Stationary-Phase Mutagenesis. Journal of bacteriology 193:236–45.

709 Denamur, E., and I. Matic. 2006. Evolution of mutation rates in bacteria. Molecular
710 microbiology 60:820–7.

711 Drake, J. W., B. Charlesworth, D. Charlesworth, and J. F. Crow. 1998. Rates of
712 spontaneous mutation. Genetics 148:1667–86.

713 Eshel, I. 1981. On the survival probability of a slightly advantageous mutant gene
714 with a general distribution of progeny size - a branching process model. Journal of
715 Mathematical Biology 12:355–362.

716 Fisher, R. A. 1930. The Genetical Theory of Natural Selection (p. 272). Clarendon
717 Press, Oxford.

718 Foster, P. L. 2007. Stress-induced mutagenesis in bacteria. Critical reviews in
719 biochemistry and molecular biology 42:373–97.

720 Funchain, P., A. Yeung, J. L. Stewart, R. Lin, M. M. Slupska, and J. H. Miller. 2000.
721 The consequences of growth of a mutator strain of *Escherichia coli* as measured by
722 loss of function among multiple gene targets and loss of fitness. Genetics 154:959–70.

723 Galhardo, R. S., P. J. Hastings, and S. M. Rosenberg. 2007. Mutation as a stress
724 response and the regulation of evolvability. Critical reviews in biochemistry and
725 molecular biology 42:399–435.

726 Gavrilets, S. 1996. On phase three of the shifting-balance theory. Evolution 50:1034–
727 1041.

728 Gentile, C. F., S.-C. Yu, S. A. Serrano, P. J. Gerrish, and P. D. Sniegowski. 2011.
729 Competition between high- and higher-mutating strains of *Escherichia coli*. Biology
730 letters 7:422–4.

731 Gessler, D. D. G. 1995. The constraints of finite size in asexual populations and the
732 rate of the ratchet. Genetical Research 66:241.

733 Giraud, A., I. Matic, O. Tenaillon, A. Clara, M. Radman, M. Fons, and F. Taddei.
734 2001a. Costs and benefits of high mutation rates: adaptive evolution of bacteria in the
735 mouse gut. Science 291:2606–8.

736 Giraud, A., M. Radman, I. Matic, and F. Taddei. 2001b. The rise and fall of mutator
737 bacteria. Current Opinion in Microbiology 4:582–585.

738 Goho, S., and G. Bell. 2000. Mild environmental stress elicits mutations affecting
739 fitness in Chlamydomonas. Proceedings of the Royal Society B: Biological Sciences
740 267:123–9.

741 Gordo, I., and F. Dionisio. 2005. Nonequilibrium model for estimating parameters of
742 deleterious mutations. Physical Review E 71:18–21.

743 Gordo, I., L. Perfeito, and A. Sousa. 2011. Fitness effects of mutations in bacteria.
744 Journal of molecular microbiology and biotechnology 21:20–35.

745 Hadany, L. 2003. Adaptive peak shifts in a heterogenous environment. Theoretical
746 Population Biology 63:41–51.

747 Hadany, L., and T. Beker. 2003. Fitness-associated recombination on rugged adaptive
748 landscapes. Journal of evolutionary biology 16:862–870.

749 Haigh, J. 1978. The accumulation of deleterious genes in a population - Muller's
750 Ratchet. Theoretical Population Biology 14:251–267.

751 Hall, L. M. C., and S. K. Henderson-Begg. 2006. Hypermutable bacteria isolated from
752 humans--a critical analysis. Microbiology (Reading, England) 152:2505–14.

753 Heidenreich, E. 2007. Adaptive mutation in *Saccharomyces cerevisiae*. Critical reviews
754 in biochemistry and molecular biology 42:285–311.

755 Henderson-Begg, S. K., D. M. Livermore, and L. M. C. Hall. 2006. Effect of
756 subinhibitory concentrations of antibiotics on mutation frequency in *Streptococcus*
757 *pneumoniae*. The Journal of antimicrobial chemotherapy 57:849–54.

758 Johnson, T., and N. H. N. H. Barton. 2002. The effect of deleterious alleles on
759 adaptation in asexual populations. Genetics 162:395–411.

760 Kang, J. M., N. M. Iovine, and M. J. Blaser. 2006. A paradigm for direct stress-induced
761 mutation in prokaryotes. The FASEB journal : official publication of the Federation
762 of American Societies for Experimental Biology 20:2476–85.

763 Katz, S., and R. Hershberg. 2013. Elevated mutagenesis does not explain the
764 increased frequency of antibiotic resistant mutants in starved aging colonies. PLoS
765 genetics 9:e1003968.

766 Kessler, D., and H. Levine. 1998. Mutator Dynamics on a Smooth Evolutionary
767 Landscape. Physical Review Letters 80:2012–2015.

768 Kibota, T. T., and M. Lynch. 1996. Estimate of the genomic mutation rate deleterious
769 to overall fitness in *E. coli*. Nature 381:694–6.

770 Kimura, M. 1967. On the evolutionary adjustment of spontaneous mutation rates.
771 Genetical Research 9:23–34.

772 Kimura, M., and T. Maruyama. 1966. The mutational load with epistatic gene
773 interactions in fitness. Genetics 54:1337–51.

774 Kivisaar, M. 2010. Mechanisms of stationary-phase mutagenesis in bacteria:
775 mutational processes in pseudomonads. FEMS microbiology letters 312:1–14.

776 Leigh, E. G. J. 1970. Natural Selection and Mutability. The American Naturalist
777 104:301–305.

778 Liberman, U., and M. W. Feldman. 1986. Modifiers of mutation rate: a general
779 reduction principle. Theoretical population biology 30:125–42.

780 Loh, E., J. J. Salk, and L. A. Loeb. 2010. Optimization of DNA polymerase mutation
781 rates during bacterial evolution. Proceedings of the National Academy of Sciences
782 107:1154–9.

783 Lynch, M., R. Bürger, D. Butcher, and W. Gabriel. 1993. The mutational meltdown in
784 asexual populations. The Journal of heredity 84:339–44.

785 Matsuba, C., D. G. Ostrow, M. P. Salomon, A. Tolani, and C. F. Baer. 2012.
786 Temperature, stress and spontaneous mutation in *Caenorhabditis briggsae* and
787 *Caenorhabditis elegans*. Biology letters 8–12.

788 Maynard Smith, J., and J. Haigh. 1974. The hitch-hiking effect of a favourable gene.
789 Genetical Research 23:23–35.

790 Montanari, S., A. Oliver, P. Salerno, A. Mena, G. Bertoni, B. Tümmler, L. Cariani, et
791 al. 2007. Biological cost of hypermutation in *Pseudomonas aeruginosa* strains from
792 patients with cystic fibrosis. Microbiology (Reading, England) 153:1445–54.

793 Moore, F. B.-G., and S. J. Tonsor. 1994. A Simulation of Wright's Shifting-Balance
794 Process: Migration and the Three Phases. Evolution 48:69.

795 Obolski, U., and L. Hadany. 2012. Implications of stress-induced genetic variation for
796 minimizing multidrug resistance in bacteria. BMC Medicine 10:1–30.

797 Otto, S. P., and T. Day. 2007. A biologist's guide to mathematical modeling in ecology
798 and evolution (p. 732). Princeton University Press.

799 Patwa, Z., and L. M. Wahl. 2008. The fixation probability of beneficial mutations.
800 Journal of the Royal Society, Interface / the Royal Society 5:1279–89.

801 Peck, S. L., S. P. Ellner, and F. Gould. 2000. Varying migration and deme size and the
802 feasibility of the shifting balance. Evolution 54:324–7.

803 Ponder, R. G., N. C. Fonville, and S. M. Rosenberg. 2005. A switch from high-fidelity
804 to error-prone DNA double-strand break repair underlies stress-induced mutation.
805 Molecular cell 19:791–804.

806 Pupo, G. M., and B. J. Richardson. 1995. Biochemical genetics of a natural population
807 of *Escherichia coli*: seasonal changes in alleles and haplotypes. Microbiology (Reading,
808 England) 141:1037–44.

809 Ram, Y., and L. Hadany. 2012. The evolution of stress-induced hypermutation in
810 asexual populations. Evolution 66:2315–28.

811 Rodriguez, G. P., N. V Romanova, G. Bao, N. C. Rouf, Y. W. Kow, and G. F. Crouse.
812 2012. Mismatch repair-dependent mutagenesis in nondividing cells. Proceedings of
813 the National Academy of Sciences 109:6153–8.

814 Rosenberg, S. M., C. Shee, R. L. Frisch, and P. J. Hastings. 2012. Stress-induced
815 mutation via DNA breaks in *Escherichia coli*: A molecular mechanism with
816 implications for evolution and medicine. BioEssays 1–8.

817 Schrag, S. J., V. Perrot, and B. R. Levin. 1997. Adaptation to the fitness costs of
818 antibiotic resistance in *Escherichia coli*. Proceedings of the Royal Society B: Biological
819 Sciences 264:1287–91.

820 Sharp, N. P., and A. F. Agrawal. 2012. Evidence for elevated mutation rates in low-
821 quality genotypes. Proceedings of the National Academy of Sciences 109:6142–6.

822 Shaw, F. H., and C. F. Baer. 2011. Fitness-dependent mutation rates in finite
823 populations. Journal of evolutionary biology 24:1677–84.

824 Shee, C., J. L. Gibson, M. C. Darrow, C. Gonzalez, and S. M. Rosenberg. 2011. Impact
825 of a stress-inducible switch to mutagenic repair of DNA breaks on mutation in
826 *Escherichia coli*. Proceedings of the National Academy of Sciences 108:13659–13664.

827 Shor, E., C. a. Fox, and J. R. Broach. 2013. The yeast environmental stress response
828 regulates mutagenesis induced by proteotoxic stress. PLoS genetics 9:e1003680.

829 Sniegowski, P. D., P. J. Gerrish, T. Johnson, and A. Shaver. 2000. The evolution of
830 mutation rates: separating causes from consequences. BioEssays 22:1057–66.

831 Sniegowski, P. D., P. J. Gerrish, and R. E. Lenski. 1997. Evolution of high mutation
832 rates in experimental populations of E. coli. Nature 387:703–5.

833 Taddei, F., M. Radman, J. Maynard Smith, B. Toupance, P.-H. Gouyon, and B.
834 Godelle. 1997. Role of mutator alleles in adaptive evolution. Nature 387:700–2.

835 Tenaillon, O., E. Denamur, and I. Matic. 2004. Evolutionary significance of stress-
836 induced mutagenesis in bacteria. Trends in microbiology 12:264–70.

837 Tenaillon, O., H. Le Nagard, B. Godelle, and F. Taddei. 2000. Mutators and sex in
838 bacteria: conflict between adaptive strategies. Proceedings of the National Academy
839 of Sciences 97:10465–70.

840 Tenaillon, O., B. Toupance, H. Le Nagard, F. Taddei, and B. Godelle. 1999. Mutators,
841 population size, adaptive landscape and the adaptation of asexual populations of
842 bacteria. Genetics 152:485–93.

Torres-Barceló, C., G. Cabot, A. Oliver, A. Buckling, and R. C. MacLean. 2013. A trade-off between oxidative stress resistance and DNA repair plays a role in the evolution of elevated mutation rates in bacteria. Proceedings of the Royal Society B: Biological Sciences 280:20130007.

Wade, M. J., and C. J. Goodnight. 1991. Wright's shifting balance theory: an experimental study. Science 253:1015–8.

Weinreich, D. M., and L. Chao. 2005. Rapid evolutionary escape by large populations from local fitness peaks is likely in nature. Evolution 59:1175–82.

Weissman, D. B., M. W. Feldman, and D. S. Fisher. 2010. The rate of fitness-valley crossing in sexual populations. Genetics 186:1389–410.

Whitlock, M. C. 1995. Variance-induced peak shifts. Evolution 49:252.

Whitlock, M. C. 1997. Founder effects and peak shifts without genetic drift: adaptive peak shifts occur easily when environments fluctuate slightly. Evolution 51:1044.

Whitlock, M. C., and P. C. Phillips. 2000. The exquisite corpse: a shifting view of the shifting balance. Trends in Ecology & Evolution 15:347–348.

Wielgoss, S., J. E. Barrick, O. Tenaillon, S. Cruveiller, B. Chane-Woon-Ming, C. Médigue, R. E. Lenski, et al. 2011. Mutation rate inferred from synonymous substitutions in a long-term evolution experiment with *Escherichia coli*. G3: Genes, Genomes, Genetics 1:183–186.

Wielgoss, S., J. E. Barrick, O. Tenaillon, M. J. Wiser, W. J. Dittmar, S. Cruveiller, B. Chane-Woon-Ming, et al. 2012. Mutation rate dynamics in a bacterial population reflect tension between adaptation and genetic load. Proceedings of the National Academy of Sciences 110:222–227.

Wright, S. 1931. Evolution in Mendelian Populations. Genetics 16:97–159.

Wright, S. 1988. Surfaces of selective value revisited. American Naturalist 131:115–123.

8. Tables

Table 1 – Model parameters and estimated values for *E. coli*

Symbol	Name	Estimate	References
s	Selection coefficient	0.001-0.03	(Kibota and Lynch 1996; Gordo et al. 2011)
H	Double mutant advantage	1-10	(Gordo et al. 2011)
U	Genomic deleterious mutation rate	0.0004-0.003	(Drake et al. 1998; Wielgoss et al. 2011)
μ	Site-specific mutation rate	$U/5000$	(Gordo et al. 2011)
τ	Fold-increase in mutation rate	1-100	(Bjedov et al. 2003; Hall and Henderson-Begg 2006)
N	Population size	10^5-10^{10}	(Pupo and Richardson 1995; Berg 1996)

9. Supporting figures

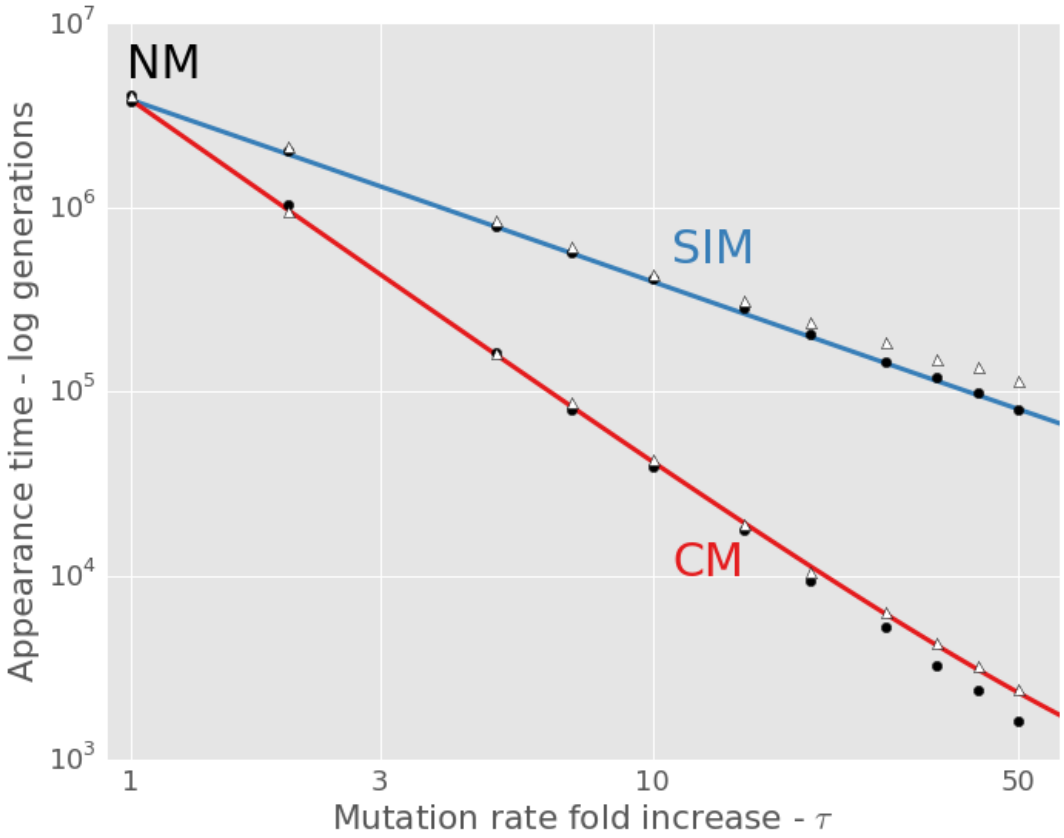

Online Figure S1 – Waiting time for the appearance of a double mutant as a function of the mutation rate fold increase τ. Normal mutagenesis (NM) is τ=1; constitutive mutagenesis (CM) in red; stress-induced mutagenesis (SIM) in blue. Lines are analytic approximations (eqs. 2, 3 in main text). Markers are means of simulation results - black circles for the standard simulations, white triangles for alternative simulations in which *AB* cannot appear on deleterious backgrounds. The standard error of the mean was too small to show. At least 1,000 simulations per point. Both axes are in log scale. The appearance time decreases as a function of τ^2 and τ with CM and SIM, respectively. Appearance time is slightly longer if *AB* only appears on unloaded background (white triangles) which explains the difference between the analytic approximations and the simulation results for SIM in Figure 2. Parameters are the same as in Figure 2.

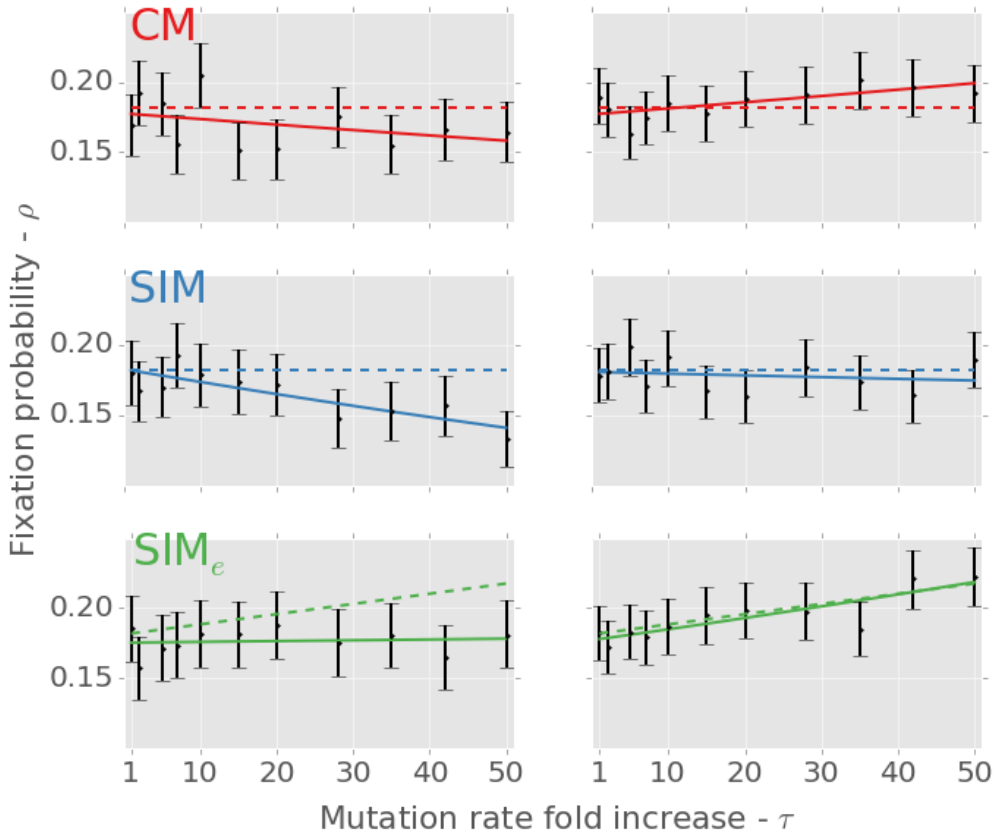

887

888 **Online Figure S2 – Fixation probability of the double mutant *AB*** as a function of the
889 mutation rate fold increase τ with three mutational strategies: constitutive mutagenesis (CM;
890 top panels in red), stress-induced mutagenesis (SIM; middle panels in blue) and stress-
891 induced mutagenesis with environmental stress (SIM$_e$; bottom panels in green; see section 3.5
892 in main text). Dashed lines are analytic approximations; black error bars represent simulation
893 results with 95% confidence interval of the mean (at least 1,000 simulations per point;
894 computed with bootstrap with 10,000 samples per point); solid lines are the logistic regression
895 lines computed from the simulation results. The three left panels are results of the standard
896 simulations. The three right panels are results of simulations in which *AB* cannot appear on
897 deleterious backgrounds - in these cases there is no significant difference between the
898 simulation results and our analytic approximations (compare solid and dashed lines;
899 regression slope tests with α=0.05). However, if *AB* can appear on a deleterious background

(left panels) then its fixation probability is lower (Johnson and Barton 2002). For example, the fixation probability of AB with a single deleterious mutation is $\rho_{AB/1} = \rho\left(1 - \frac{1}{H(1-s)}\right) < \rho$. In addition, the figure shows that SIM_e has a higher fixation probability than CM and SIM: the green lines, representing SIM_e, are always higher than the red and blue lines representing CM and SIM. Parameters are the same as in Figure 2.